

## A Favorable Case Where an Experimental Electron Density Analysis Offers a Lead for Understanding a Specific Fluxional Process Observed in Solution

Yannick Ortin,<sup>†</sup> Noël Lugan,<sup>\*,†</sup> Sébastien Pillet,<sup>‡</sup> Mohammed Souhassou,<sup>‡</sup> Claude Lecomte,<sup>\*,‡</sup> Karine Costuas,<sup>§</sup> and Jean-Yves Saillard<sup>\*,§</sup>

Laboratoire de Chimie de Coordination du CNRS, 205 route de Narbonne, 31077 Toulouse Cedex 4, France, Laboratoire de Cristallographie et de Modélisation des Matériaux Minéraux et Biologiques, Faculté des Sciences, Université Henri Poincaré, 54506 Vandoeuvre-Lès-Nancy Cedex, France, and Laboratoire de Chimie du Solide et Inorganique, Institut de Chimie Moléculaire de Rennes, Université de Rennes 1, 35042 Rennes Cedex, France

Received July 25, 2005

A topological analysis of the electron density in the ketene complex ( $\eta^5\text{-MeC}_5\text{H}_4$ )(CO)<sub>2</sub>Mn[ $\eta^2\text{-O=C=C}(\mu\text{-}\eta^2\text{-C}\equiv\text{CPh})\text{Co}_2(\text{CO})_6$ ]Ph indicates a predisposition for the carbene component of the ketene ligand to bind the neighboring C atom of the adjacent CO ligand.

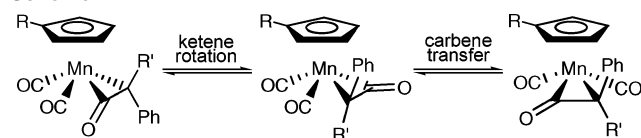
Current advances in instrumentation and analytical methods have rendered experimental electron density (ED) studies a very valuable tool for investigating electronic structures and bonding schemes within molecules and materials, including organometallic complexes.<sup>1</sup>

We have recently reported that the carbonyl of the ketene ligand in manganese complexes of the type ( $\eta^5\text{-RC}_5\text{H}_4$ )(CO)<sub>2</sub>Mn[ $\eta^2\text{-O=C=C}(\text{R}')\text{Ph}$ ] exchanges rapidly [NMR time scale] with the carbonyl ligands.<sup>2</sup> A key step in this unprecedented dynamic behavior involves a rapid transfer of the ketene's carbene component, C(R')Ph, onto an adjacent CO ligand (Scheme 1).

Having in hand high-quality single crystals of the ketene complex ( $\eta^5\text{-MeC}_5\text{H}_4$ )(CO)<sub>2</sub>Mn[ $\eta^2\text{-O=C=C}(\mu\text{-}\eta^2\text{-C}\equiv\text{CPh})\text{-Co}_2(\text{CO})_6$ ]Ph (**1**), we envisioned that a topological analysis of the experimental ED might provide mechanistic clues on the above dynamic process.

An accurate high-resolution X-ray data set was thus collected on **1** at 100 K up to  $2\theta_{\text{max}} = 137^\circ$  (Mo K $\alpha$

Scheme 1



radiation).<sup>3</sup> The experimental ED was derived from the X-ray data using the MoPro program<sup>4a</sup> based on the multipole model as formulated by Hansen and Coppens.<sup>4b</sup> For the sake of comparison, a theoretical model of the ED was computed by carrying out density functional theory (DFT) single-point calculations on the X-ray structure of **1**.<sup>5</sup> Subsequent topological analysis of the experimental and theoretical EDs based on Bader's quantum theory of atoms in molecules (AIM)<sup>6</sup> was achieved using the NEWPROP<sup>7</sup> and XAIM<sup>8</sup> programs.

The structure of **1** shown in Figure 1 is naturally analogous to the previously reported one (from a 298 K data set).<sup>2</sup> The most striking geometrical feature is the occurrence of a dissymmetrical coordination of the ketene ligand about Mn, with the Mn1–C3 distance of 1.9572(4) Å being significantly

- (3) Crystal data for **1**: C<sub>30</sub>H<sub>17</sub>Co<sub>2</sub>MnO<sub>9</sub>,  $M = 694.24$ , triclinic, space group  $P\bar{1}$ ,  $a = 9.2994(5)$  Å,  $b = 10.1733(6)$  Å,  $c = 14.6154(7)$  Å,  $\alpha = 98.870(4)^\circ$ ,  $\beta = 90.080(4)^\circ$ ,  $\gamma = 97.201(4)^\circ$ ,  $V = 1355.08(12)$  Å<sup>3</sup>,  $T = 100(1)$  K,  $Z = 2$ ,  $F_{000} = 696$ ,  $D_c = 1.702$  Mg/m<sup>3</sup>,  $\mu = 1.728$  mm<sup>-1</sup>. A total of 119 756 Bragg reflections were collected at 100 K up to  $\sin \theta/\lambda = 1.31$  Å<sup>-1</sup> on an Oxford Diffraction Xcalibur diffractometer equipped with a Sapphire CCD detector. After decay and absorption corrections (by faces indexing), a set of 35 022 unique reflections [ $R_{\text{int}}(I) = 0.021$ , 68% of data  $5.3^\circ < 2\theta < 136.7^\circ$ , (redundancy) = 3.7] were used for a multipolar refinement based on the Hansen and Coppens formalism.<sup>4</sup> The multipole expansion was truncated at the hexadecapole level for Mn and Co atoms and at the octupole level for the O and C atoms. The H–C bond-directed dipole was introduced for the H atoms. The C–H bond distances were constrained to typical neutron values. The refinement of 1025 parameters against 33 924 observed reflections ( $I > 0$ ) converged to  $R = 0.0430$  and  $R_w = 0.0222$ ; GOF = 1.86.

- (4) (a) Jelsch, C.; Guillot, B.; Lagoutte, A.; Lecomte, C. *J. Appl. Crystallogr.* **2004**, *38*, 38. (b) Hansen, N. K.; Coppens, P. *Acta Crystallogr.* **1978**, *A34*, 909.

\* To whom correspondence should be addressed. E-mail: lugan@lcc-toulouse.fr (N.L.), lecomte@lcm3b.u-nancy.fr (C.L.), saillard@univ-rennes1.fr (J.-Y.S.).

<sup>†</sup> Laboratoire de Chimie de Coordination du CNRS.

<sup>‡</sup> Université Henri Poincaré.

<sup>§</sup> Université de Rennes 1.

- (1) (a) Koritsanszky, T. S.; Coppens, P. *Chem. Rev.* **2001**, *101*, 1583. (b) Macchi, P.; Sironi, A. *Coord. Chem. Rev.* **2003**, *238*, 383. (c) Farrugia, L. J.; Mallinson, P. R.; Stewart, B. *Acta Crystallogr.* **2003**, *B59*, 234. (d) Pillet, S.; Wu, G.; Kulsomphob, V.; Harvey, B. G.; Ernst, R. D.; Coppens, P. *J. Am. Chem. Soc.* **2003**, *125*, 1937. (e) Lecomte, C.; Aubert, E.; Legrand, V.; Porcher, F.; Pillet, S.; Guillot, B.; Jelsch, C. *Z. Kristallogr.* **2005**, *220*, 373.
- (2) Ortin, Y.; Coppel, Y.; Lugan, N.; Mathieu, R.; McGlinchey, M. J. *Chem. Commun.* **2001**, 2636.

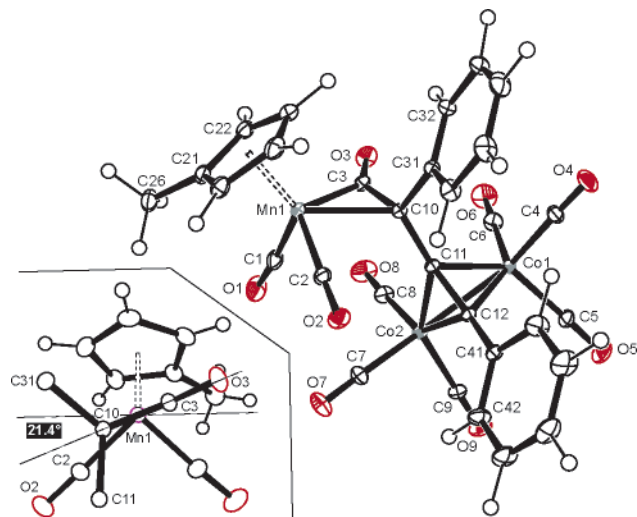


**Figure 1.** Perspective view of complex **1**. Inset on the left side: view of the ketene complex component of **1** seen from the Mn1–{centroid of the C3–C10 bond} axis.

shorter than the Mn1–C10 distance [2.1989(4) Å;  $\Delta d = 0.2417(8)$  Å]. Actually, the Mn1–C3 distance in **1** lies in the low limits of the Mn–C bond distance within a  $\pi$  ligand coordinated to the  $(\eta^5\text{-RC}_5\text{H}_4)(\text{CO})_2\text{Mn}$  fragment.<sup>9</sup>

Bond paths (bp's) and bond critical points (bcp's) revealed by the topology of the experimental ED for complex **1** are shown in Figure 2a. In the following, we will focus on the Mn– $\eta^2\text{-C,C}$ -ketene complex facet of **1** where the fluxional process sits.<sup>10</sup> Table 1 lists salient parameters at selected bcp's. Topological parameters derived from the theoretical calculation are in good agreement with those obtained experimentally, despite the somehow common discrepancies for the Laplacian of the carbonyl bonds.<sup>1c,11</sup> Within the Mn1–C3–C10 triangle, the AIM analysis shows two bcp's only, one between Mn1 and C3 and one between C3 and C10 (Figure 2b). Surprisingly, no bcp between Mn1 and C10 could be detected. Indeed, in their pioneering experimental ED-based AIM analysis of a metal/ $\pi$ -bonded ligand com-

plex, namely, Ni(1,5-COD)<sub>2</sub>, Macchi et al.<sup>12</sup> have found, for a typical ring structure topology for the NiC<sub>2</sub> triangles with two bcp's between Ni and each C atom, one bcp between the two C atoms and one ring critical point (rcp).<sup>13</sup> Going from such a ring structure to the present situation, one has to consider that the elongation of Mn1–C10 has caused the associated bcp to vanish owing to merging with the rcp into a singular point in  $\rho(r)$  through a phenomenon corresponding to a bond fission in the AIM framework.<sup>14</sup> According to the molecular graph, the Mn–ketene interaction would be described as  $\eta^1$ ; however, the Mn1–C3 and C3–C10 bp's are slightly outwardly curved, which indicates that these two bonds belong to a more complex system.<sup>15</sup> A comparison of the parameters at the M–C bcp's within **1** and Ni(1,5-COD)<sub>2</sub><sup>11</sup> also reveals that ED at the Mn1–C3 bcp of **1** is relatively high [0.72 e/Å<sup>3</sup> versus an average of 0.55 e/Å<sup>3</sup> at the Ni–C bcp's] and that the ellipticity of Mn1–C3 is very small [0.10 versus 2–5 at the Ni–C bcp's]. In addition,  $\rho(r)$  at the bcp between C3 and C10 is relatively low, and using the same rough approximation as that of Macchi et al.,<sup>12</sup> we get an approximate bond order value of only 1.16 for that bond versus 1.77 for the coordinated C=C bonds in Ni(1,5-COD)<sub>2</sub>. In the present complex, the lengthening, or opening, of Mn1–C10 seems to be concomitant with the reinforcement of the Mn1–C3 bond, which tends to acquire a  $\sigma$  character, and a decrease in the C3–C10 bond order to practically unity.

Back to the solid-state structure of **1**, a closer look reveals that the ketene ligand is off by 21.4° from the so-called horizontal coordination mode (Figure 1, inset), which can be expected, based on electronic grounds, for an ketene ligand  $\eta^2\text{-C,C}$ -bonded to a CpML<sub>2</sub>-type metal fragment.<sup>16</sup> Actually, such a rotation brings C10 at 2.5020(4) Å only from C2, thus favoring the possible buildup of a bonding interaction between these two atoms.

Although no bcp could ever be evidenced between C2 and C10, the Laplacian of the ED, which has been shown to highlight local charge concentrations (cc's) and local charge depletions, is very informative. In the vicinity of C10, four local cc's are observed. Three of them are pointing toward the neighboring C3, C11, and C31 atoms, as is expected for covalent C–C bonds. The fourth cc, however, is clearly pointing toward the carbon atom C2 of the adjacent carbonyl ligand (Figure 2c). We believe that this reflects a predisposition for CC bond formation, with this cc being indeed available for the formation of a covalent chemical bond with C2.

- (5) DFT calculations were carried out with the Amsterdam Density Functional package, version 2002.01, with the BP86 functional (SCM, Theoretical Chemistry, Vrije Universiteit, Amsterdam, The Netherlands; <http://www.scm.com>). The atomic basis set used is a triple- $\zeta$  Slater-type orbital extended with a single- $\zeta$  polarization function basis (basis TZP of ADF). A frozen-core approximation was applied for the orbitals up to 4p for Mn and Co and 1s for C and O.
- (6) Bader, R. F. W. *Atoms in Molecules: A Quantum Theory*; Clarendon Press: New York, 1990.
- (7) Souhassou, M.; Blessing, R. H. *J. Appl. Crystallogr.* **1999**, *32*, 210.
- (8) Ortiz, J. C.; Jané, C. B. *XAIM–X Atoms in Molecules Interface*, version 1.0; Universitat Rovira I Virgili: Tarragona, Spain.
- (9) (a) Examination of the CSD reveals an average of 2.133 Å for the (Mn–C) bonds [with C belonging to the ( $\eta^2\text{-C,C}$ -ligand)] within complexes of the type  $(\eta^5\text{-RC}_5\text{H}_4)\text{Mn}(\eta^2\text{-C,C}$ -ligand), with a minimum of 1.947(3) Å associated with  $(\eta^5\text{-MeC}_5\text{H}_4)(\text{CO})_2\text{Mn}(\eta^2\text{-C,C-OCH=C=CHO})$ .<sup>9b</sup> (b) Franck-Neumann, M.; Neff, D.; Nouali, H.; Martina, D.; de Cian, A. *Synlett* **1994**, 657.
- (10) (a) The topology of the ED of the  $[\eta^2\text{-C,C-alkyne}]Co_2(CO)_6$  moiety, although not the primary matter of the present Communication, presents some features worth mentioning: (i) no bcp is observed between the Co atoms, as for CO-bridged-only Co–Co bonds;<sup>10b</sup> (ii) both Co<sub>2</sub> triangles show a typical ring structure with three bcp's and their associated rcp, with the bp being inwardly curved. (b) Macchi, P.; Garlaschelli, L.; Martinengo, S.; Sironi, A. *J. Am. Chem. Soc.* **1999**, *121*, 10428.
- (11) For instance, see: Macchi, P.; Garlaschelli, L.; Sironi, A. *J. Am. Chem. Soc.* **2002**, *124*, 14173.

- (12) Macchi, P.; Proserpio, D. M.; Sironi, A. *J. Am. Chem. Soc.* **1998**, *120*, 1447.
- (13) Macchi et al. pointed out that a ring structure topology could be revealed only if the multipole expansion for the C atoms were extended up to the hexadecapole level.<sup>12</sup> In the present case, attempts to do so did not either reveal a ring structure topology or improve the model.
- (14) (a) Bader, R. F. W.; Nguyen-Dang, T. T.; Tal, Y. *Rep. Prog. Phys.* **1981**, *44*, 893 (b) Cremer, D.; Kraka, E. *J. Am. Chem. Soc.* **1985**, *107*, 3800.
- (15) Koritsanzky, T.; Buschmann, J.; Luger, P. *J. Phys. Chem.* **1996**, *100*, 10547.
- (16) (a) Schilling, B. E. R.; Hoffmann, R.; Lichtenberger, D. L. *J. Am. Chem. Soc.* **1979**, *101*, 585. (b) Caulton, K. G. *Coord. Chem. Rev.* **1981**, *38*, 1.

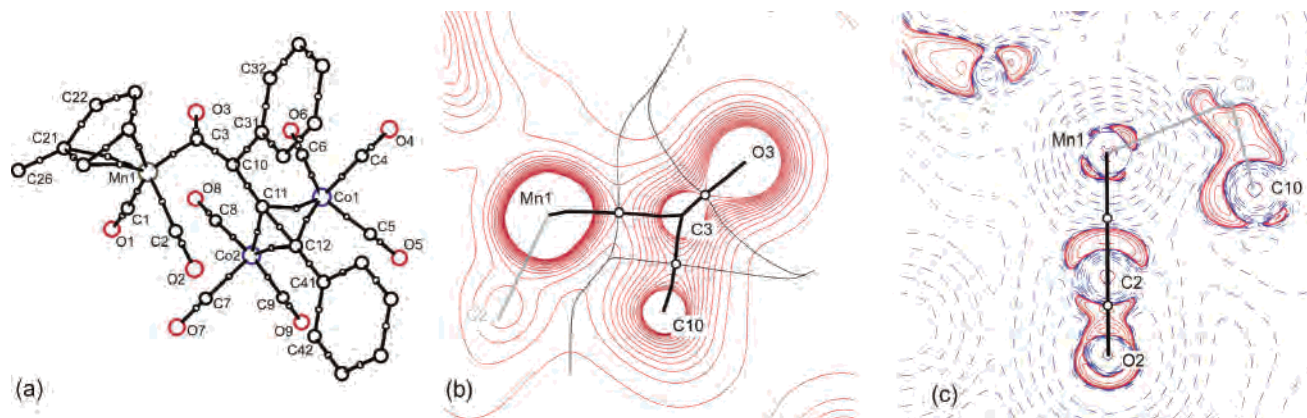


**Figure 2.** (a) bp's and bcp's within complex **1** (H atoms have been omitted for the sake of clarity). Small open dots are bcp's. (b) Total experimental ED  $\rho(r)$  ( $0.2 \text{ e}/\text{\AA}^3$  isocontours;  $0.1\text{--}2.9 \text{ e}/\text{\AA}^3$  range), bond and atomic basins, in the Mn1–C3–C10 plane. Small open dots are bcp's. (c) Experimental  $\nabla^2\rho(r)$  function in the Mn1–C2–C10 plane. Contours are drawn at  $0.000, \pm 2.0 \times 10n, \pm 4.0 \times 10n,$  and  $\pm 8.0 \times 10n \text{ e}/\text{\AA}^5$  levels, where  $n = 0, -3, \pm 2,$  and  $\pm 1$ .

**Table 1.** Topological Properties of the Experimental and Theoretical (Italics) ED at Relevant bcp's<sup>a</sup>

bond	<i>d</i>	<i>d</i> <sub>1</sub>	<i>d</i> <sub>2</sub>	$\nabla^2\rho(r)$	$\rho(r)$	$\epsilon$
Mn1–C1	1.7933(4)	0.884	0.910	12.25	1.03	0.04
		0.874	0.918	12.74	1.03	0.05
Mn1–C2	1.8173(4)	0.876	0.942	12.11	0.97	0.07
		0.892	0.923	11.93	0.99	0.12
Mn1–C3	1.9572(4)	0.927	1.033	7.24	0.72	0.09
		0.943	1.001	6.49	0.82	0.15
C1–O1	1.1578(6)	0.391	0.767	3.22	3.22	0.00
		0.404	0.749	–2.58	3.31	0.00
C2–O2	1.1490(5)	0.390	0.759	–0.94	3.31	0.01
		0.402	0.745	–1.58	3.36	0.00
C3–O3	1.2025(5)	0.407	0.796	–8.00	2.91	0.05
		0.424	0.777	–8.34	2.95	0.01
C3–C10	1.4381(4)	0.738	0.702	–13.22	1.86	0.10
		0.699	0.737	–8.49	2.00	0.17

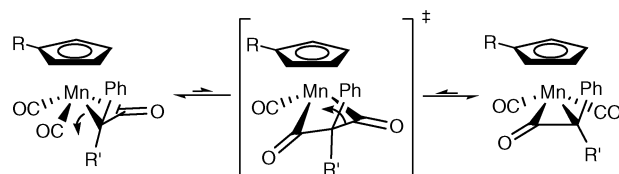
<sup>a</sup> *d* is the interatomic distance ( $\text{\AA}$ ); *d*<sub>1</sub> and *d*<sub>2</sub> are the distances ( $\text{\AA}$ ) from the bcp to each of the linked atoms, respectively;  $\rho(r)$ ,  $\nabla^2\rho(r)$ , and  $\epsilon$  are the ED ( $\text{e}/\text{\AA}^3$ ), the Laplacian of the ED ( $\text{e}/\text{\AA}^5$ ), and the ellipticity of the bond.

Actually, in good agreement with the above observations, the DFT-computed Mulliken overlap population between C2 and C10 (+0.014) is indicative of a weak bonding interaction, or at least of the absence of the usual interligand repulsion. Also noteworthy and fully consistent with the absence of bcp between Mn and C10 is the corresponding overlap population (0.093), which is much smaller than the Mn1–C3 one (0.270).

Now, what are these observations coming from an experimental study on the solid state telling us about the carbene transfer process occurring in solution? The geometry of the molecule, the topology of the ED and of the Laplacian of the ED, and the Mulliken overlap population analysis show, in particular, the weakening of Mn1–C10, the decrease in the bond order C3–C10, and the possible buildup of a bond between C2 and C10. Taken altogether, these data are all consistent with the idea that the intramolecular hopping of the ketene's carbene component onto the adjacent carbonyl takes place via a transient 16-electron metallacycle, as depicted in Scheme 2.

Although their  $\pi$ -bonding abilities are somewhat different, carbonyl and carbene ligands have sufficient similarities for being considered to some extent as isolobal analogues. Taking also into account the isolobal analogy between

### Scheme 2



ketenes and alkenes, we are inclined to draw a parallel between the present CO to CO carbene transfer and the “Chauvin” mechanism, which governs olefin metathesis by transition-metal complexes.<sup>17</sup> Finally, the structure “frozen” in the solid state would be close enough to the transition state to express some of its character. The observed molecular graph for this frozen structure results from the balance of all forces acting on the atoms of the molecule (Ehrenfest forces). It is easily understood that, in liquid, forces generated by the crystal packing are left, allowing the dynamic fluxional process to occur.

A detailed analysis of the theoretical ED redistribution and the evolution of the theoretical molecular graph, along the whole reaction path of carbene transfer, is needed to clarify the proposal. A DFT investigation of this reaction in a dynamic point of view is currently underway in our laboratories and will be published in due course.

**Acknowledgment.** N.L. thanks the “Mission Formation Permanente” of the DR14-CNRS for sponsoring his sabbatical leave at the LCM<sup>3</sup>B in Nancy, France, and Dr. Guy Lavigne for stimulating discussions. DFT calculations have been carried out at the IDRIS-CNRS computing center (Orsay, France). We also thank Dr. Mathias Meyer from Oxford Diffraction Ltd. for helpful advice and Ethyl Corp. (Richmond, VA) for a generous gift of  $(\eta^5\text{-MeC}_5\text{H}_4)\text{Mn}(\text{CO})_3$ .

**Supporting Information Available:** Full details on the data collection and on the multipole refinement, including tables and maps (CIF and PDF). This material is available free of charge via the Internet at <http://pubs.acs.org>.

IC051239P

(17) (a) Eisenstein, O.; Hoffmann, R.; Rossi, A. R. *J. Am. Chem. Soc.* **1981**, *103*, 5582. (b) Suresh, C. H.; Koga, N. *Organometallics* **2004**, *23*, 76.